

# Imaging and dynamics for physical and life sciences

## Directly imaging the localisation and photosensitization properties of the pan-mTOR inhibitor, AZD2014, in living cancer cells

**A.R. Ahmed** (Central Laser Facility, Research Complex at Harwell, STFC Rutherford Appleton Laboratory, Harwell Campus, Didcot, UK; Larch House, Woodlands Business Park, Breckland, Linford Wood, Milton Keynes MK14 6FG, UK)

**A. Candeo, S.R. Needham, S.W. Botchway, A.W. Parker** (Central Laser Facility, Research Complex at Harwell, STFC Rutherford Appleton Laboratory, Harwell Campus, Didcot, UK)

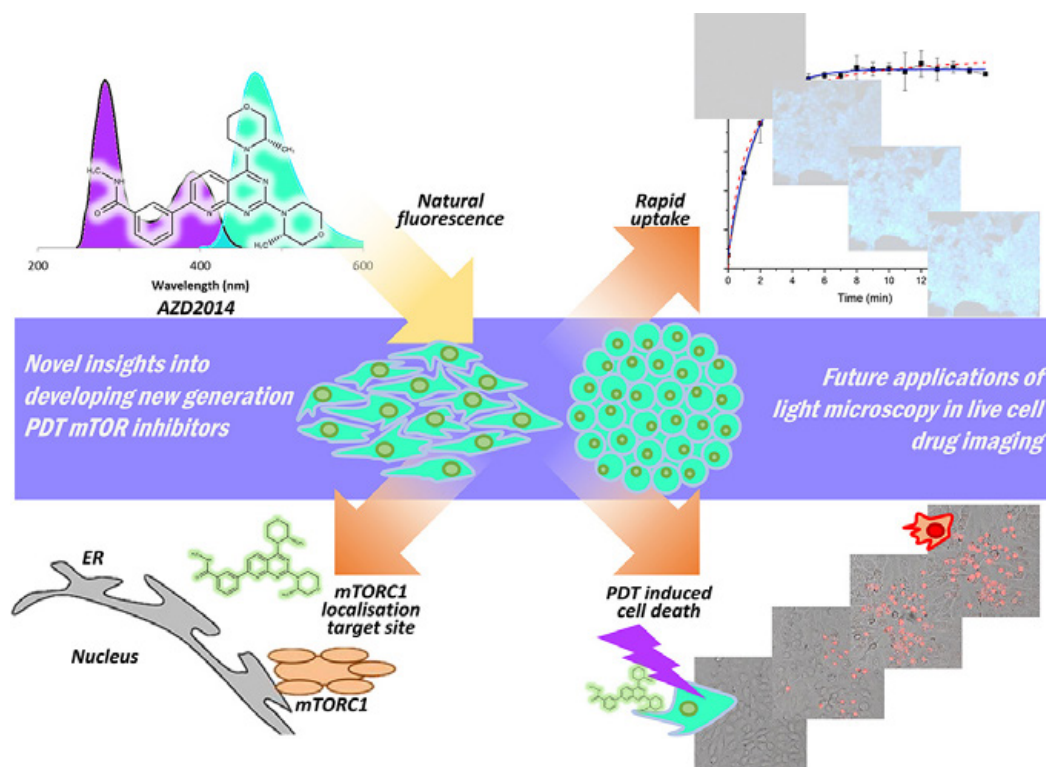
**S. D'Abrantes** (Central Laser Facility, Research Complex at Harwell, STFC Rutherford Appleton Laboratory, Harwell Campus, Didcot, UK; CRUK/MRC Oxford Institute for Radiation Oncology, University of Oxford, Gray Laboratories, UK)

**R.B. Yadav** (Evotec (UK) Ltd, Milton Park, Abingdon, UK)

The range of cellular functions the mechanistic target of rapamycin (mTOR) protein performs makes it an attractive drug target for cancer therapy. However, the cellular localisation and mode of action of second generation inhibitors of mTOR is poorly understood despite the level of attention there is in targeting the mTOR protein. We have therefore studied the properties of the pan-mTOR inhibitor AZD2014, an ideal candidate to study because it is naturally fluorescent, characterising its photochemical properties in solution phase (DMSO, PBS and BSA) and within living cells, where it localises within both the nucleus and the cytoplasm but with different excited state lifetimes of 4.8 (+/- 0.5) and 3.9 (+/- 0.4) ns respectively. We measure the uptake of the inhibitor AZD2014 (7  $\mu$ M) in monolayer HEK293 cells occurring with a half-life of 1 min but observe complex behaviour for 3D spheroids with the core of the

spheroid showing a slower uptake and a slow biphasic behaviour at longer times. From a cellular perspective using fluorescence lifetime imaging microscopy AZD2014 was found to interact directly with GFP-tagged mTORC1 proteins including the downstream target, S6K1. We observe light sensitive behaviour of the cells containing AZD2014 which leads to cell death, in both monolayer and spheroids cells, demonstrating the potential of AZD2014 to act as a possible photodynamic drug under both single photon and multiphoton excitation and discuss its use as a photosensitizer. We also briefly characterise another pan-mTOR inhibitor, INK128.

Reproduced from Ahmed, Abdullah R., et al. "Directly imaging the localisation and photosensitization properties of the pan-mTOR inhibitor, AZD2014, in living cancer cells." *Journal of Photochemistry and Photobiology B: Biology* (2020): 112055, under the terms of the Creative Commons Attribution 4.0 International (CC BY 4.0) License. doi: 10.1016/j.jphotobiol.2020.112055



Contacts: S.W. Botchway (stan.botchway@stfc.ac.uk)  
A.W. Parker (a.w.parker@stfc.ac.uk)

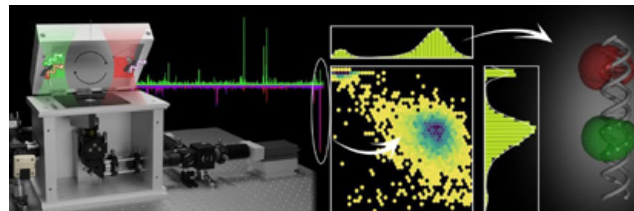
## The smfBox is an open-source platform for single-molecule FRET

**B. Ambrose, J.M. Baxter, J. Cully, M. Willmott, J. Shewring, M. Aldering, T.D. Craggs** (Sheffield Institute for Nucleic Acids, Department of Chemistry, University of Sheffield, UK)  
**E.M. Steele, A. Cadby** (Department of Physics, University of Sheffield, UK)

**B.C. Bateman, M. Martin-Fernandez** (Central Laser Facility, Research Complex at Harwell, STFC Rutherford Appleton Laboratory, Harwell Campus, Didcot, UK)

Single-molecule Förster Resonance Energy Transfer (smFRET) is a powerful technique capable of resolving both relative and absolute distances within and between structurally dynamic biomolecules. High instrument costs, and a lack of open-source hardware and acquisition software have limited smFRET's broad application by non-specialists. Here, we present the smfBox, a cost-effective confocal smFRET platform, providing detailed build instructions, open-source acquisition software, and full validation, thereby democratising smFRET for the wider scientific community.

Reproduced from Ambrose, B., Baxter, J.M., Cully, J. et al. The smfBox is an open-source platform for single-molecule FRET. *Nat Commun* 11, 5641 (2020), published by Springer Nature, under the terms of a Creative Commons Attribution 4.0 International License. doi: 10.1038/s41467-020-19468-4



The smfBox (left) is a robust, affordable instrument for single-molecule FRET experiments, built from machined aluminium and off-the-shelf components. Molecules diffuse through a confocal volume and are alternately excited by a green and red lasers (left top), generating FRET and stoichiometry values, which are plotted on a 2D histogram (centre). The FRET efficiencies can be related to the structure of the biomolecule under investigation (right).

Contact: T.D. Craggs (t.craggs@sheffield.ac.uk)

## Preparation of polymer gold nanoparticle composites with tunable plasmon coupling and their application as SERS substrates

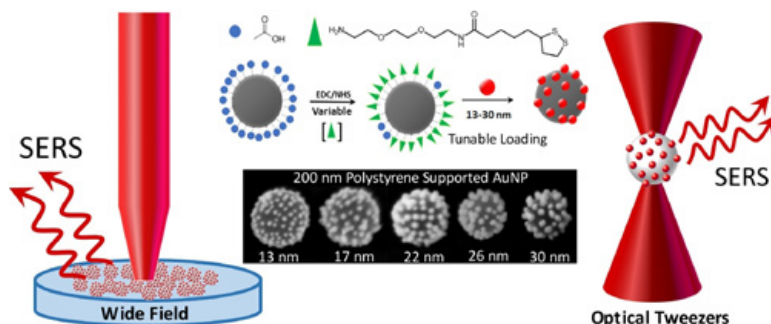
**S.A. Belhout, F.R. Baptista, S.J. Devereux, S.J. Quinn** (School of Chemistry, University College Dublin, Republic of Ireland)

**A.W. Parker, A.D. Ward** (Central Laser Facility, Research Complex at Harwell, STFC Rutherford Appleton Laboratory, Harwell Campus, Didcot, UK)

The controlled surface functionalisation of polystyrene beads (200 nm) with a lipionic acid derivative is used to assemble composites with between 4 to 20% loadings of citrate stabilised gold nanoparticles (13 nm–30 nm), which exhibit variable optical properties arising from interactions of the nanoparticle surface plasmon resonance (SPR). The decrease in average interparticle distance at higher loadings results in a red-shift in the SPR wavelength, which is well described by a universal ruler equation. The composite particles are shown to act as good SERS substrates for the standard analyte 4-mercaptophenol. The direct assessment of the SERS activity for individual composite particles solution is achieved by Raman optical

tweezer measurements on 5.3  $\mu\text{m}$  composite particles. These measurements show an increase in performance with increasing AuNP size. Importantly, the SERS activity of the individual particles compares well with the bulk measurements of samples deposited on a surface, indicating that the SERS activity arises primarily from the composite and not due to composite–composite interactions. In both studies the optimum SERS response is obtained with 30 nm AuNPs.

Reproduced from S. A. Belhout, F. R. Baptista, S. J. Devereux, A. W. Parker, A. D. Ward and S. J. Quinn, Preparation of polymer gold nanoparticle composites with tunable plasmon coupling and their application as SERS substrates. *Nanoscale*, 2019, 11, 19884–19894. doi: 10.1039/C9NR05014K with permission from the Royal Society of Chemistry.



Contact: S.J. Quinn (susan.quinn@ucd.ie)

## Adaptive lipid immiscibility and membrane remodeling are active functional determinants of primary ciliogenesis

**M. Bernabé-Rubio** (Department of Cell Biology and Immunology, Centro de Biología Molecular Severo Ochoa, Consejo Superior de Investigaciones Científicas and Universidad Autónoma de Madrid, Spain; King's College London Centre for Stem Cells and Regenerative Medicine, Guy's Campus, London, UK)

**M. Bosch-Fortea** (Department of Cell Biology and Immunology, Centro de Biología Molecular Severo Ochoa, Consejo Superior de Investigaciones Científicas and Universidad Autónoma de Madrid, Spain; Institute of Bioengineering and School of Engineering and Materials Science, Queen Mary University of London, UK)

**M.A. Alonso** (Department of Cell Biology and Immunology, Centro de Biología Molecular Severo Ochoa, Consejo Superior de Investigaciones Científicas and Universidad Autónoma de Madrid, Spain)

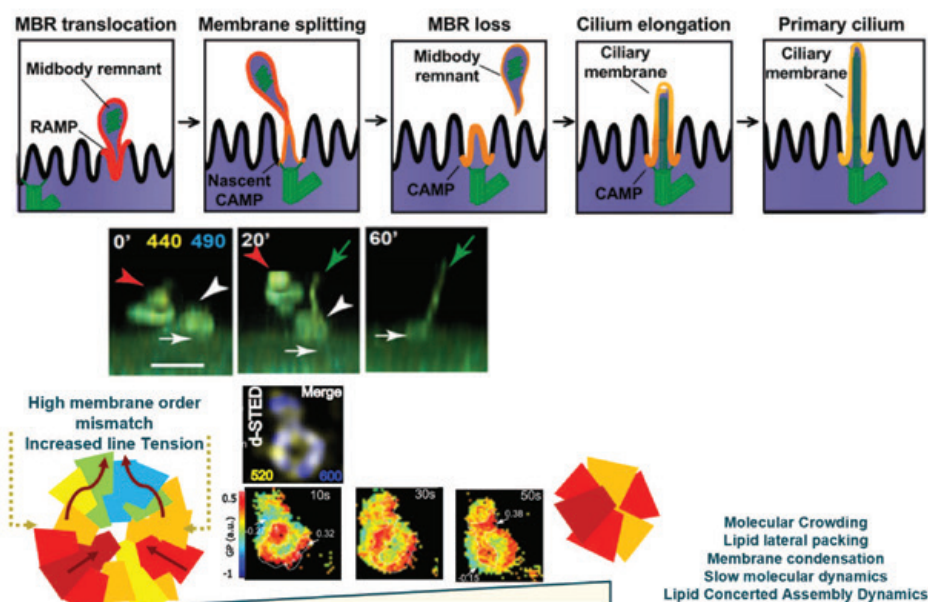
**E. García** (Central Laser Facility, Research Complex at Harwell, STFC Rutherford Appleton Laboratory, Harwell Campus, Didcot, UK; CR-UK Beatson Institute, Glasgow, UK)

**J. Bernadino de la Serna** (Central Laser Facility, Research Complex at Harwell, STFC Rutherford Appleton Laboratory, Harwell Campus, Didcot, UK; National Heart and Lung Institute, Imperial College London, UK; NIHR Imperial Biomedical Research Centre, London, UK)

Lipid liquid–liquid immiscibility and its consequent lateral heterogeneity have been observed under thermodynamic equilibrium in model and native membranes. However, cholesterol-rich membrane domains, sometimes referred to as lipid rafts, are difficult to observe spatiotemporally in live cells. Despite their importance in many biological processes, robust evidence for their existence remains elusive. This is mainly due to the difficulty in simultaneously determining their chemical composition and physicochemical nature, whilst spatiotemporally resolving their nanodomain lifetime and molecular dynamics. In this study, a bespoke method based on super-resolution stimulated emission depletion (STED) microscopy and raster imaging correlation spectroscopy (RICS) is used to overcome this issue. This methodology, laser interleaved confocal RICS and STED-RICS (LICSR),

enables simultaneous tracking of lipid lateral packing and dynamics at the nanoscale. Previous work indicated that, in polarized epithelial cells, the midbody remnant licenses primary cilium formation through an unidentified mechanism. LICSR shows that lipid immiscibility and its adaptive collective nanoscale self-assembly are crucial for the midbody remnant to supply condensed membranes to the centrosome for the biogenesis of the ciliary membrane. Hence, this work poses a breakthrough in the field of lipid biology by providing compelling evidence of a functional role for liquid ordered-like membranes in primary ciliogenesis.

Reproduced from Bernabé-Rubio, M., Bosch-Fortea, M., García, E., Bernardino de la, J., Alonso, M. A., Adaptive Lipid Immiscibility and Membrane Remodeling Are Active Functional Determinants of Primary Ciliogenesis. *Small Methods* 2021, 5, 2000711, published by Wiley-VCH GmbH, under the terms of the Creative Commons Attribution-NonCommercial-NoDerivs License. doi: 10.1002/smt.202000711



Contact: M.A. Alonso (maalonso@cbm.csic.es)

## Combining Multicolor FISH with Fluorescence Lifetime Imaging for Chromosomal Identification and Chromosomal Sub Structure Investigation

**A. Bhartiya** (London Centre for Nanotechnology, University College London, UK; Research Complex at Harwell, STFC Rutherford Appleton Laboratory, Harwell Campus, Didcot, UK)  
**I. Robinson** (London Centre for Nanotechnology, University College London, UK; Condensed Matter Physics and Materials Science Division, Brookhaven National Lab, Upton, NY, USA)

**M. Yusuf** (London Centre for Nanotechnology, University College London, UK; Research Complex at Harwell, STFC Rutherford Appleton Laboratory, Harwell Campus, Didcot, UK; Centre for Regenerative Medicine and Stem Cell Research, Aga Khan University, Karachi, Pakistan)  
**S.W. Botchway** (Central Laser Facility, Research Complex at Harwell, STFC Rutherford Appleton Laboratory, Harwell Campus, Didcot, UK)

Understanding the structure of chromatin in chromosomes during normal and diseased state of cells is still one of the key challenges in structural biology. Using DAPI staining alone together with Fluorescence lifetime imaging (FLIM), the environment of chromatin in chromosomes can be explored. Fluorescence lifetime can be used to probe the environment of a fluorophore such as energy transfer, pH and viscosity. Multicolor FISH (M-FISH) is a technique that allows individual chromosome identification, classification as well as assessment of the entire genome. Here we describe a combined approach using DAPI as a DNA environment sensor together with FLIM and M-FISH to understand the nanometer structure of all 46 chromosomes in the nucleus covering the entire human genome at the single cell level. Upon DAPI binding to DNA minor groove followed by fluorescence lifetime measurement and imaging by multiphoton excitation, structural differences in the chromosomes can be studied and observed. This manuscript provides a blow by blow account of the protocol required to perform M-FISH-FLIM of whole chromosomes.

Reproduced from Bhartiya A, Robinson I, Yusuf M and Botchway SW (2021) Combining Multicolor FISH with Fluorescence Lifetime Imaging for Chromosomal Identification and Chromosomal Sub Structure Investigation. *Front. Mol. Biosci.* 8:631774, under the terms of the Creative Commons Attribution License (CC BY). doi: 10.3389/fmolb.2021.631774



Multicolor FISH performed on the chromosome spread, after FLIM imaging, followed by karyotype as shown in image.

Contacts: M. Yusuf (yusuf.mohammed@ucl.ac.uk)  
 S.W. Botchway (stan.botchway@stfc.ac.uk)

## Porous Carbon Microparticles as Vehicles for the Intracellular Delivery of Molecules

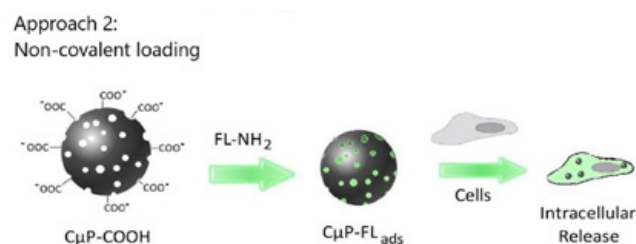
**L.M. Magno, D.T. Hinds, S.J. Quinn** (School of Chemistry, University College Dublin, Ireland)  
**P. Duffy, P.E. Colavita** (School of Chemistry, Trinity College Dublin, Ireland)

**A.D. Ward, S.W. Botchway, R.B. Yadav** (Central Laser Facility, Research Complex at Harwell, STFC Rutherford Appleton Laboratory, Harwell Campus, Didcot, UK)

In this study the application of porous carbon microparticles for the transport of a sparingly soluble material into cells is demonstrated. Carbon offers an intrinsically sustainable platform material that can meet the multiple and complex requirements imposed by applications in biology and medicine. Porous carbon microparticles are attractive as they are easy to handle and manipulate and combine the chemical versatility and biocompatibility of carbon with a high surface area due to their highly porous structure. The uptake of fluorescently labelled microparticles by cancer (HeLa) and normal human embryonic kidney (HEK293) cells was monitored by confocal fluorescence microscopy. In this way the influence of particle size, surface functionalization and the presence of transfection agent on cellular uptake were studied. In the presence of transfection agent both large (690 nm) and small microparticles (250 nm) were readily internalized by both cell lines. However, in absence of the transfection agent the uptake was influenced by particle size and surface PEGylation with the smaller nanoparticle size being delivered. The ability of microparticles to deliver a fluorescein dye model cargo was also demonstrated in normal (HEK293) cell line. Taken together, these results

indicate the potential use of these materials as candidates for biological applications.

Reproduced from Magno LM, Hinds DT, Duffy P, Yadav RB, Ward AD, Botchway SW, Colavita PE and Quinn SJ (2020) Porous Carbon Microparticles as Vehicles for the Intracellular Delivery of Molecules. *Front. Chem.* 8:576175, under the terms of the Creative Commons Attribution (CC BY) License. doi: 10.3389/fchem.2020.576175



Negatively charged CμP-COOH particles were non-covalently loaded with a highly fluorescent amino-fluorescein dye to prepare CμP-FLads. The ability of these particles to deliver their model cargo to cells was then investigated.

Contact: S.J. Quinn (susan.quinn@ucd.ie)

## A small molecule inhibitor of HER3: a proof-of-concept study

**A. Colomba, J. Claus** (Protein Phosphorylation Laboratory, The Francis Crick Institute, London, UK)

**M. Fitzek** (Hit Discovery, Discovery Sciences, R&D, AstraZeneca, Macclesfield, UK)

**R. George, S. Kjaer** (Structural Biology Science Technology Platform, The Francis Crick Institute, London, UK)

**G. Weitsman, T. Ng** (Richard Dimpleby Department of Cancer Research, School of Cancer and Pharmaceutical Sciences, King's College London, Guy's Campus, London, UK)

**S. Roberts, L. Zanetti-Domingues, M. Hirsch, D.J. Rolfe, M. Martin-Fernandez** (Central Laser Facility, Research Complex at Harwell, STFC Rutherford Appleton Laboratory, Harwell Campus, Didcot, UK)

**S. Mehmood, A.P. Snijders** (Protein Analysis and Proteomics Science Technology Platform, The Francis Crick Institute, London, UK)

**A. Madin** (Hit Discovery, Discovery Sciences, R&D, AstraZeneca, Cambridge, UK)

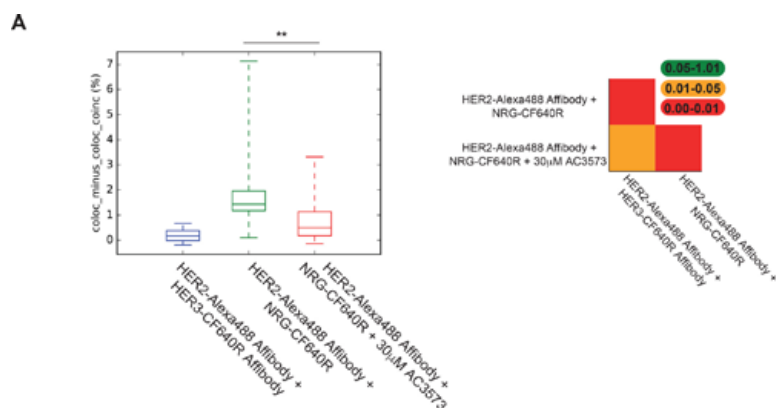
**D.M. Smith** (Emerging Innovations Unit, Discovery Sciences, R&D, AstraZeneca, Cambridge, UK)

**P.J. Parker** (Protein Phosphorylation Laboratory, The Francis Crick Institute, London, UK; CRUK KHP Centre, School of Cancer and Pharmaceutical Sciences, King's College London, Guy's Campus, London, UK)

Despite being catalytically defective, pseudokinases are typically essential players of cellular signalling, acting as allosteric regulators of their active counterparts. Deregulation of a growing number of pseudokinases has been linked to human diseases, making pseudokinases therapeutic targets of interest. Pseudokinases can be dynamic, adopting specific conformations critical for their allosteric function. Interfering with their allosteric role, with small molecules that would lock pseudokinases in a conformation preventing their productive partner interactions, is an attractive therapeutic strategy to explore. As a well-known allosteric activator of epidermal growth factor receptor family members, and playing a major part in cancer progression, the pseudokinase HER3 is a relevant context in which to address the potential

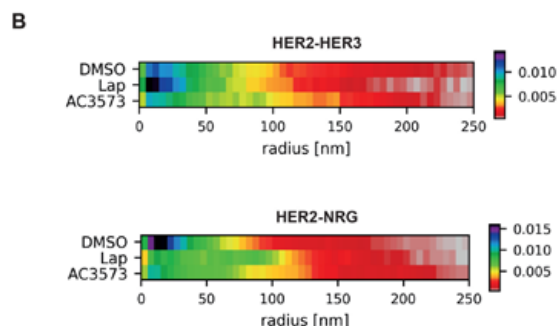
of pseudokinases as drug targets for the development of allosteric inhibitors. In this proof-of-concept study, we developed a multiplex, medium-throughput thermal shift assay screening strategy to assess over 100,000 compounds and identify selective small molecule inhibitors that would trap HER3 in a conformation which is unfavourable for the formation of an active HER2–HER3 heterodimer. As a proof-of-concept compound, AC3573 bound with some specificity to HER3 and abrogated HER2–HER3 complex formation and downstream signalling in cells. Our study highlights the opportunity to identify new molecular mechanisms of action interfering with the biological function of pseudokinases.

Reproduced from A. Colomba et al., *Biochem J* (2020) 477 (17): 3329–3347, published by Portland Press Limited on behalf of the Biochemical Society and distributed under the Creative Commons Attribution License 4.0 (CC BY). doi: 10.1042/BCJ20200496



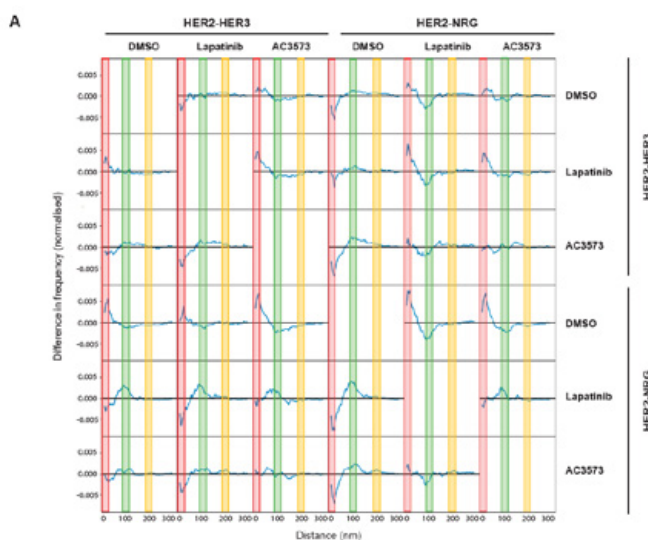
Left: AC3573 compound abrogates the formation of the active HER2–HER3 heterodimer.

(A) Left: the percentage of tracks where HER2 and HER3 molecules spent at least five 50 ms frames together within <1 pixel (pairwise particle colocalisation fraction) in CHO cells with and without treatment with AC3573. (B) Heat map of the probability of the distance of nearest HER2 neighbour of HER3. Cluster measurements from STORM data taken from SK-BR-3 cells labelled with HER2-Alexa488 Affibody and HER3-CF640R SE Affibody (HER2–HER3) or NRG-CF640R SE (HER2–NRG) ± 1 μM lapatinib or 30 μM AC3573 compound.



Right: AC3573 compound disrupts HER2–HER3 heterodimers but does not induce HER3 homodimers.

(A) Differences in probability of HER2–HER3 nearest neighbour distances. Cluster measurements from STORM data taken from SK-BR-3 cells labelled with HER2-Alexa488 Affibody and HER3-CF640R SE Affibody (HER2–HER3) or NRG-CF640R SE (HER2–NRG) ± 1 μM lapatinib or 30 μM AC3573 compound. Graphs show near neighbour distribution of HER2 and HER3 molecules as Y condition (right-hand side) – X condition (top). A positive difference indicates that it is more likely to find a HER2 at the corresponding distance from a HER3 under Y condition than under X condition.



Contact: P.J. Parker (peter.parker@crick.ac.uk)

## Super-Resolution Fluorescence Microscopy Reveals Clustering Behaviour of *Chlamydia pneumoniae*'s Major Outer Membrane Protein

**A. E. Danson** (School of Biological Sciences, University of Reading, UK; Diamond Light Source, Harwell Science and Innovation Campus, Didcot, UK; Research Complex at Harwell, STFC Rutherford Appleton Laboratory, Harwell Campus, Didcot, UK)

**A. McStea, L. Wang, M. L. Martin-Fernandez** (Central Laser Facility, Research Complex at Harwell, Science and Technology Facilities Council, Rutherford Appleton Laboratory, Harwell, Didcot, Oxford OX11 0QX, UK)

**A. Y. Pollitt, K. Watson, S. MacIntyre** (School of Biological Sciences, University of Reading, Berkshire RG6 6AS, UK)

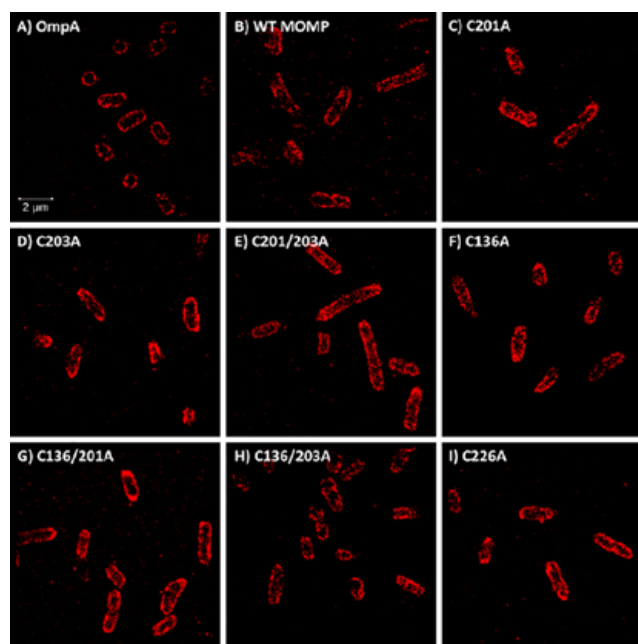
**M. A. Walsh** (Diamond Light Source, Harwell Science and Innovation Campus, Oxfordshire OX11 0DE, UK; Research Complex at Harwell, Harwell Science and Innovation Campus, Oxfordshire OX11 0FA, UK)

**I. Moraes** (Research Complex at Harwell, Harwell Science and Innovation Campus, Oxfordshire OX11 0FA, UK; National Physical Laboratory, Teddington TW11 0LW, UK)

*Chlamydia pneumoniae* is a Gram-negative bacterium responsible for a number of human respiratory diseases and linked to some chronic inflammatory diseases. The major outer membrane protein (MOMP) of *Chlamydia* is a conserved immunologically dominant protein located in the outer membrane, which, together with its surface exposure and abundance, has led to MOMP being the main focus for vaccine and antimicrobial studies in recent decades. MOMP has a major role in the chlamydial outer membrane complex through the formation of intermolecular disulphide bonds, although the exact interactions formed are currently unknown. Here, it is proposed that due to the large number of cysteines available for disulphide bonding, interactions occur between cysteine-rich pockets as opposed to individual residues. Such pockets were identified using a MOMP homology model with a supporting low-resolution ( $\sim 4 \text{ \AA}$ ) crystal structure. The localisation of MOMP in the *E. coli* membrane was assessed using direct stochastic optical reconstruction microscopy (dSTORM), which showed a decrease in membrane clustering with cysteine-rich regions containing two mutations. These results indicate that disulphide bond formation was not disrupted by single mutants located in the cysteine-dense regions and was compensated by neighbouring cysteines within the pocket in support of this cysteine-rich pocket hypothesis.

Reproduced from Danson AE, McStea A, Wang L, Pollitt AY, Martin-Fernandez ML, Moraes I, Walsh MA, MacIntyre S, Watson KA. Super-Resolution Fluorescence Microscopy Reveals Clustering Behaviour of *Chlamydia pneumoniae*'s Major Outer Membrane Protein. *Biology*. 2020; 9(10):344. under the Creative Commons Attribution License 4.0 (CC BY) doi: 10.3390/biology9100344

Contact: K.A. Watson (k.a.watson@reading.ac.uk)



High-resolution dSTORM images reveal wild-type MOMP to be highly clustered. Double mutants C201/203A and C136/201A reduce the clustering of MOMP most significantly, suggesting that within cysteine-rich regions, a compensatory mechanism is occurring whereby neighbouring cysteine residues can continue to form intermolecular disulphide bonds in the absence of the most important cysteine residue and effectively form the protective cysteine rich chlamydial outer membrane complex.

## A Targeted and Tuneable DNA Damage Tool Using CRISPR/Cas9

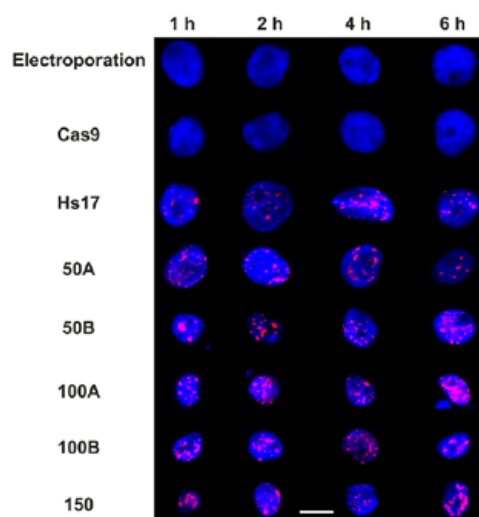
I. Emmanouilidis, Y. Hari-Gupta, P.J.I. Ellis (School of Biosciences, University of Kent, Canterbury, UK)

N. Fili, A.W. Cook, Á. Dos Santos, C.P. Toseland (Department of Oncology and Metabolism, University of Sheffield, UK)

L. Wang, M. Martin-Fernandez (Central Laser Facility, Research Complex at Harwell, STFC Rutherford Appleton Laboratory, Harwell Campus, Didcot, UK)

Mammalian cells are constantly subjected to a variety of DNA damaging events that lead to the activation of DNA repair pathways. Understanding the molecular mechanisms of the DNA damage response allows the development of therapeutics which target elements of these pathways. Double-strand breaks (DSB) are particularly deleterious to cell viability and genome stability. Typically, DSB repair is studied using DNA damaging agents such as ionising irradiation or genotoxic drugs. These induce random lesions at non-predictive genome sites, where damage dosage is difficult to control. Such interventions are unsuitable for studying how different DNA damage recognition and repair pathways are invoked at specific DSB sites in relation to the local chromatin state. The RNA-guided Cas9 (CRISPR-associated protein 9) endonuclease enzyme is a powerful tool to mediate targeted genome alterations. Cas9-based genomic intervention is attained through DSB formation in the genomic area of interest. Here, we have harnessed the power to induce DSBs at defined quantities and locations across the human genome, using custom-designed promiscuous guide RNAs, based on in silico predictions. This was achieved using electroporation of recombinant Cas9-guide complex, which provides a generic, low-cost and rapid methodology for inducing controlled DNA damage in cell culture models.

Reproduced from Emmanouilidis I, Fili N, Cook AW, Hari-Gupta Y, dos Santos Á, Wang L, Martin-Fernandez ML, Ellis PJI, Toseland CP. A Targeted and Tuneable DNA Damage Tool Using CRISPR/Cas9. *Biomolecules*. 2021; 11(2):288, under the terms of the Creative Commons Attribution License (CC BY 4.0). doi: 10.3390/biom11020288



Time course of Cas9-induced DNA damage. Example widefield images of MCF10a cells stained for DNA with Hoechst (blue) and  $\gamma$ H2AX (red). Electroporation is a control for background signals. Cas9 refers to electroporation of Cas9 alone. Hs17 is the crRNA predicted to cut the genome at 17 locations [16], while 50A/B, 100A/B and 150 are our designed promiscuous crRNA which cut at 50, 100 and 150 predicted sites, respectively. 'A' versions are GC-selective sequences while 'B' versions are AT-selective. The timing is measured from electroporation onwards. Scale bar is 10  $\mu$ m.

Contacts: P.J.I. Ellis (p.j.i.ellis@kent.ac.uk) C. Toseland (c.toseland@sheffield.ac.uk)

## Using Mie scattering to determine the wavelength-dependent refractive index of polystyrene beads with changing temperature

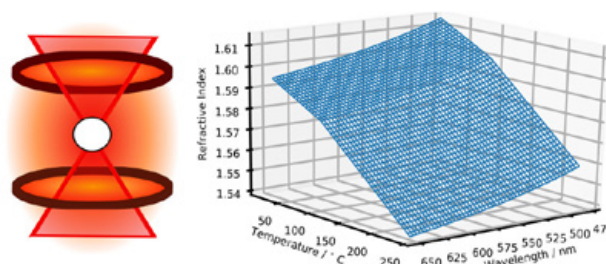
M.R. McGrory (Central Laser Facility, Research Complex at Harwell, STFC Rutherford Appleton Laboratory, Harwell Campus, Didcot, UK; Department of Earth Sciences, Royal Holloway University of London, Egham, UK)

A.D. Ward (Central Laser Facility, Research Complex at Harwell, STFC Rutherford Appleton Laboratory, Harwell Campus, Didcot, UK)

M.D. King (Department of Earth Sciences, Royal Holloway University of London, Egham, UK)

Polystyrene beads are often used as test particles in aerosol science. Here, a contact-less technique is reported for determining the refractive index of a solid aerosol particle as a function of wavelength and temperature (20–234°C) simultaneously. Polystyrene beads with a diameter of 2  $\mu$ m were optically trapped in air in the central orifice of a ceramic heating element, and Mie spectroscopy was used to determine the radius and refractive index (to precisions of 0.8 nm and 0.0014) of eight beads as a function of heating and cooling. Refractive index,  $n$ , as a function of wavelength,  $\lambda$  (0.480–0.650  $\mu$ m), and temperature,  $T$ , in centigrade, was found to be  $n = 1.5753 - (1.7336 \times 10^{-4})T + (9.733 \times 10^{-3})\lambda^{-2}$  in the temperature range  $20 < T < 100^\circ\text{C}$  and  $n = 1.5877 - (2.9739 \times 10^{-4})T + (9.733 \times 10^{-3})\lambda^{-2}$  in the temperature range  $100 < T < 234^\circ\text{C}$ . The technique represents a step change in measuring the refractive index of materials across an extended range of temperature and wavelength in an absolute manner and with high precision.

Reproduced from M.R. McGrory, A.D. Ward and M.D. King, *J. Phys. Chem. A* 2020, 124, 9617–9625, © 2020 American Chemical Society, under the terms of a Creative Commons CC-BY license. doi: 10.1021/acs.jpca.0c06121



Contact: A.D. Ward (andy.ward@stfc.ac.uk)

## Mononuclear ruthenium(II) theranostic complexes that function as broad-spectrum antimicrobials in therapeutically resistant pathogens through interaction with DNA

**K.L. Smitten** (Department of Chemistry, University of Sheffield, UK; Department of Molecular Biology and Biotechnology, University of Sheffield, UK)

**E.J. Thick, J.A. Thomas** (Department of Chemistry, University of Sheffield, UK)

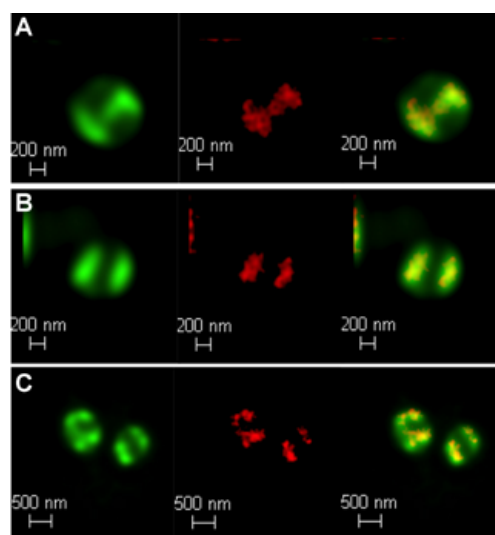
H.M. Southam, S.J. Foster (Department of Molecular Biology and Biotechnology, University of Sheffield, UK)

**J. Bernadino de la Serna** (National Heart and Lung Institute, Faculty of Medicine, Imperial College London, UK; Central Laser Facility, Research Complex at Harwell, STFC Rutherford Appleton Laboratory, Harwell Campus, Didcot, UK)

Six luminescent, mononuclear ruthenium(II) complexes based on the tetrapyrrophenazine (tpphz) and dipyrrophenazine (dppz) ligands are reported. The therapeutic activities of the complexes against Gram-negative bacteria (*E. coli*, *A. baumannii*, *P. aeruginosa*) and Gram-positive bacteria (*E. faecalis* and *S. aureus*) including pathogenic multi- and pan-drug resistant strains were assessed. Estimated minimum inhibitory and bactericidal concentrations show the activity of the lead compound is comparable to ampicillin and oxacillin in therapeutically sensitive strains and this activity was retained in resistant strains. Unlike related dinuclear analogues the lead compound does not damage bacterial membranes but is still rapidly taken up by both Gram-positive and Gram-negative bacteria in a glucose independent manner. Direct imaging of the complexes through super-resolution nanoscopy and transmission electron microscopy reveals that once internalized the complexes' intracellular target for both Gram-negative and Gram-positive strains is bacterial DNA. Model toxicity screens showed the compound is non-toxic to *Galleria mellonella* even at exposure concentrations that are orders of magnitude higher than the bacterial MIC.

Reproduced from K. L. Smitten, E. J. Thick, H. M. Southam, J. Bernadino de la Serna, S. J. Foster and J. A. Thomas, *Chem. Sci.*, 2020, 11, 8828, doi: 10.1039/D0SC03410J, with permission from the Royal Society of Chemistry under the terms of the CC BY-NC 3.0 licence

Contact: J.A. Thomas (james.thomas@sheffield.ac.uk)



Localization of  $4^{2+}$  in *S. aureus* SH1000 cells visualized through laser scanning confocal microscopy, d-LCSM, (green, left) and stimulated emission depletion nanoscopy, STED, (red, middle) and overlay image (right) at; (A) 20 min, (B) 60 min and (C) 120 min. Cells imaged using the emission of  $4^{2+}$  on excitation at 470 nm with a white light laser and a 470 nm notch filter. STED effect was obtained by employing a 770 nm depletion laser, and a 780 nm vortex phase plate. Both d-LCSM and d-STED images were processed using Huygens software (SVI).

## Serial cryoFIB/SEM Reveals Cytoarchitectural Disruptions in Leigh Syndrome Patient Cells

**Y. Zhu** (Division of Structural Biology, Wellcome Trust Centre for Human Genetics, University of Oxford, UK)

**P. Zhang** (Division of Structural Biology, Wellcome Trust Centre for Human Genetics, University of Oxford, UK; Department of Structural Biology, University of Pittsburgh School of Medicine, USA; Electron Bio-Imaging Centre, Diamond Light Source, Harwell Science and Innovation Campus, Didcot, UK)

**D. Sun, J. Ning, X. Fu** (Department of Structural Biology, University of Pittsburgh School of Medicine, USA)

**A. Schertel** (Carl Zeiss Microscopy GmbH, Zeiss Customer Center Europe, Oberkochen, Germany)

**P.P. Gwo** (Department of Psychiatry, University of Pittsburgh, USA)

**A.M. Watson** (Department of Cell Biology, University of Pittsburgh, USA)

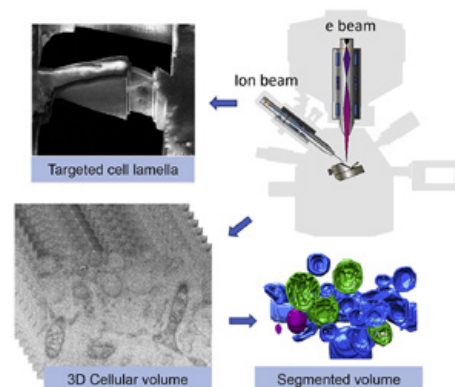
**L.C. Zanetti-Domingues, M.L. Martin-Fernandez** (Central Laser Facility, Research Complex at Harwell, STFC Rutherford Appleton Laboratory, Harwell Campus, Didcot, UK)

**Z. Freyberg** (Department of Psychiatry, University of Pittsburgh, USA; Department of Cell Biology, University of Pittsburgh, USA)

The advancement of serial cryoFIB/SEM offers an opportunity to study large volumes of near-native, fully hydrated frozen cells and tissues at voxel sizes of 10 nm and below. We explored this capability for pathologic characterization of vitrified human patient cells by developing and optimizing a serial cryoFIB/SEM volume imaging workflow. We demonstrate profound disruption of subcellular architecture in primary fibroblasts from a Leigh syndrome patient harboring a disease-causing mutation in USMG5 protein responsible for impaired mitochondrial energy production.

Reproduced from Zhu, Yanan et al. "Serial cryoFIB/SEM Reveals Cytoarchitectural Disruptions in Leigh Syndrome Patient Cells." *Structure*. vol. 29,1 (2021): 82-87.e3. under the terms of the Creative Commons CC BY 4.0 License. doi: 10.1016/j.str.2020.10.003

Contact: P. Zhang (peijun@strubi.ox.ac.uk)



## Operando Kerr gated Raman spectroscopy of lithium insertion into graphite enables high state of charge diagnostics

L.J. Hardwick, A.R. Neale, D.C. Milan, F. Braga (Stephenson Institute for Renewable Energy, Department of Chemistry, University of Liverpool, UK)

I.V. Sazanovich (Central Laser Facility, Research Complex at Harwell, STFC Rutherford Appleton Laboratory, Harwell Campus, Didcot, UK)

Operando electrochemical Kerr gated Raman spectroscopy measurements are reported for the first time to track the lithium insertion/extraction processes in a graphite-based negative electrode for Li-ion batteries. At high depths of lithiation from  $\text{Li}_{0.5}\text{C}_6$  to  $\text{LiC}_6$ , large fluorescence/emission signals swamp the weaker Raman scattering effect in conventional Raman spectroscopy, making it difficult to track material changes at high states of

charge. The efficacy of the Kerr gate in suppressing strong fluorescence/emission signals, combined with the dedicated design of the operando spectroelectrochemical cell (Figure 1), facilitated continued detection of the changing graphitic Raman bands even at high depths of lithiation to fully intercalated  $\text{LiC}_6$  (Figure 2). This creates the opportunity to interrogate high states of charge in graphitic negative electrodes for Li-ion batteries.

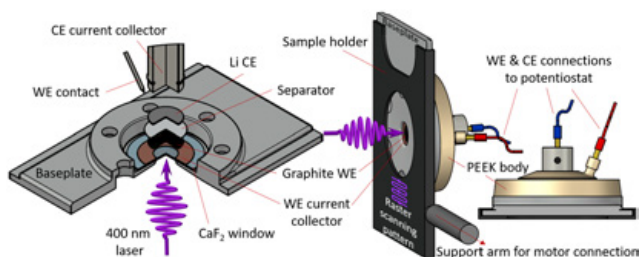


Figure 1: A schematic of the operando Raman cell assembly. The cell (left), and WE and CE connections, were sealed using PEEK body of the ECC-Opto cell (EL-Cell) and the Kerr gate Raman sample holder system (right) attached to the motor system (not shown) that provides the raster scanning motion during spectra collection.

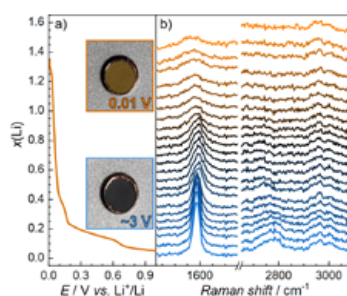


Figure 2: (a) Voltage profile of the graphite electrode and (b) the operando Kerr gated Raman spectra (stacked as a function of  $x(\text{Li})$ ) collected at 2 ps delay times showing the primary G and 2D graphite bands at 1580 and 2780  $\text{cm}^{-1}$ , respectively (electrolyte bands at ca. 2980  $\text{cm}^{-1}$ ). Spectra are stacked as a function of the depth of lithiation ( $x(\text{Li})$ ). Inset images in a-i) show images of the electrode before and after full lithiation to  $\text{LiC}_6$ .

Contact: L.J. Hardwick (hardwick@liverpool.ac.uk)

## Temperature-Jump Time Resolved 2D-IR Spectroscopy of DNA Hairpin Unfolding

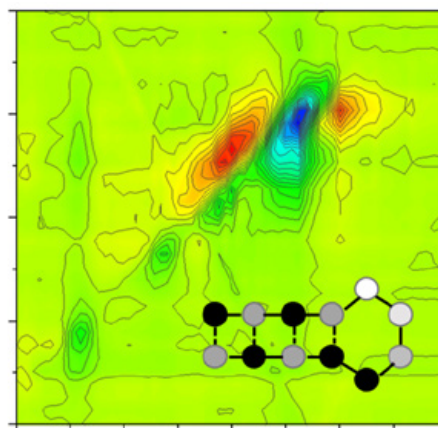
C.P. Howe, B. Procacci, D.J. Shaw, N.T. Hunt (Department of Chemistry, University of York, UK)

G.M. Greetham, M. Towrie, A.W. Parker (Central Laser Facility, STFC Rutherford Appleton Laboratory, Harwell Campus, Didcot, UK)

The ULTRA T-jump-infrared spectroscopy instrument has been extended to include the use of two-dimensional infrared (2D-IR) spectroscopy, to probe the melting dynamics of DNA hairpins in real time.

Dynamic changes in nucleic acid macromolecular structures are central to biological function, and the hairpin studied features a tetraloop motif commonly found in RNA-based ribozymes and synthetic nucleic acid aptamer molecules.

We demonstrate that T-jump-2D-IR spectroscopy on the ULTRA spectrometer has sufficient sensitivity, as well as scale and duration of the temperature jump, to enable detection of hairpin melting. This experiment establishes proof of concept for more detailed studies of the hairpin melting process, that will lead to enhanced understanding of nucleic acid structure and dynamics in solution.



T-jump-2D-IR difference spectrum showing effects of DNA hairpin melting

Contact: N.T. Hunt (neil.hunt@york.ac.uk)

# Manganese-Mediated C–H Bond Activation of Fluorinated Aromatics and the *ortho*-Fluorine Effect: Kinetic Analysis by *In Situ* Infrared Spectroscopic Analysis and Time-Resolved Methods

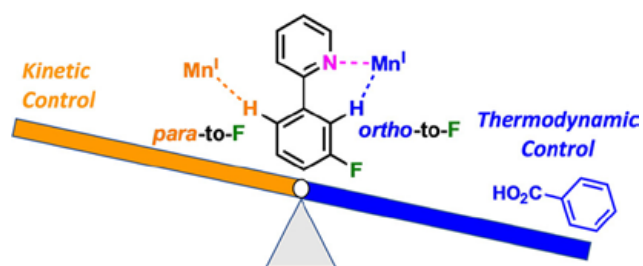
J.M. Lynam, I.J.S. Fairlamb, L.A. Hammarback, A.L. Bishop, C. Jordan, G. Athavan, J.B. Eastwood, T.J. Burden, J.T.W. Bray, F. Clarke, A. Whitwood (Department of Chemistry, University of York, UK)

A. Robinson, J.-P. Krieger (Sygenta Crop Protection AG, Mönchwil, Switzerland)  
I.P. Clark, M. Towrie (Central Laser Facility, STFC Rutherford Appleton Laboratory, Harwell Campus, Didcot, UK)

Insights into the factors controlling the site selectivity of transition metal-catalyzed C–H bond functionalization reactions are vital to their successful implementation in the synthesis of complex target molecules. The introduction of fluorine atoms into substrates has the potential to deliver this selectivity. In this study, we employ spectroscopic and computational methods to demonstrate how the “*ortho*-fluorine effect” influences the kinetic and thermodynamic control of C–H bond activation in manganese(I)-mediated reactions. The C–H bond activation of fluorinated *N,N*-dimethylbenzylamines and fluorinated 2-phenylpyridines by benzyl manganese(I) pentacarbonyl  $\text{BnMn}(\text{CO})_5$  leads to the formation of cyclomanganated tetracarbonyl complexes (**2a–b** and **4a–e**), which all exhibit C–H bond activation *ortho*-to-fluorine. Corroboration of the experimental findings with density functional theory methods confirms that a kinetically controlled irreversible  $\sigma$ -complex-assisted metathesis mechanism is operative in these reactions. The addition of benzoic acid results in a mechanistic switch, so that cyclomanganation proceeds through a reversible AMLA-6 mechanism (kinetically and thermodynamically controlled). These stoichiometric findings are critical to catalysis, particularly subsequent insertion of a suitable acceptor substrate into

the C–Mn bond of the regioisomeric cyclomanganated tetracarbonyl complex intermediates. The employment of time-resolved infrared spectroscopic analysis allowed for correlation of the rates of terminal acetylene insertion into the C–Mn bond with the relative thermodynamic stability of the regioisomeric complexes. Thus, more stable manganacycles, imparted by an *ortho*-fluorine substituent, exhibit a slower rate of terminal acetylene insertion, whereas a *para*-fluorine atom accelerates this step. A critical factor in governing C–H bond site selectivity under catalytic conditions is the generation of the regioisomeric cyclomanganated intermediates, rather than their subsequent reactivity toward alkyne insertion.

Reproduced with permission from ACS Catal. 2022, 12, 2, 1532–1544. Copyright © 2022 American Chemical Society. doi: 10.1021/acscatal.1c05477



Contacts: J.M. Lynam (jason.lynam@york.ac.uk)  
I.J.S. Fairlamb (ian.fairlamb@york.ac.uk)

## Dynamics around a hydrogen bond – The dynamics of UV excited acetic acid dimers

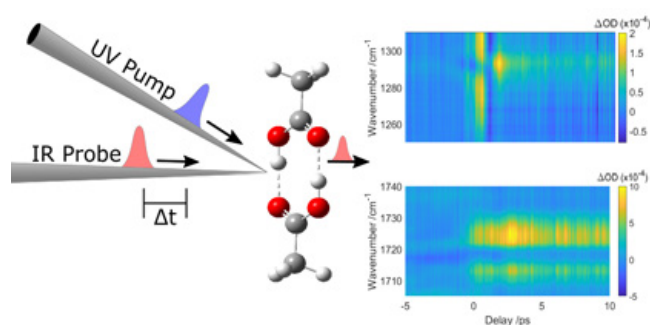
E. Plackett, R.S. Minns (School of Chemistry, University of Southampton, UK)  
 H. McGhee, R. Ingle (Department of Chemistry, University College London, UK)  
 G.M. Greetham, G. Karras, I.V. Sazanovich (Central Laser Facility, Research Complex at Harwell, STFC Rutherford Appleton Laboratory, Harwell Campus, Didcot, UK)

We measure the transient infrared absorption spectrum of UV excited acetic acid dimers. The measurements cover vibrational modes related to the ring structure of the dimer and highlight the stabilising effects of the hydrogen bonds and their effect on the excited state dynamics.

The results suggest that absorption at 200 nm leads to population of the  $S_2$  state and dynamics that change the hydrogen bonded region that stabilises the molecule against dissociation. In the excited state, the dimer initially skews and then undergoes internal conversion to  $S_1$  and buckles from the originally planar ring structure, to form a new stable configuration in the  $S_1$  excited state. The buckled structure then relaxes back to the electronic ground state, reforming the planar ground state dimer structure.

Contact: R.S. Minns (r.s.minns@soton.ac.uk)

C. Robertson, A. De Matos Loja, M. Patterson (Institute of Chemical Sciences, School of Engineering and Physical Sciences, Heriot-Watt University, Edinburgh, UK)



Left: Schematic representation of the experiment, where a pump pulse electronically excites the acetic acid dimer. The resulting dynamics are probed via changes in the infrared absorption spectrum as a function of pump-probe delay.

Right: Representative spectra around the carbonyl stretch ( $1720\text{ cm}^{-1}$ ) and the ring wag ( $1290\text{ cm}^{-1}$ ) vibrations.

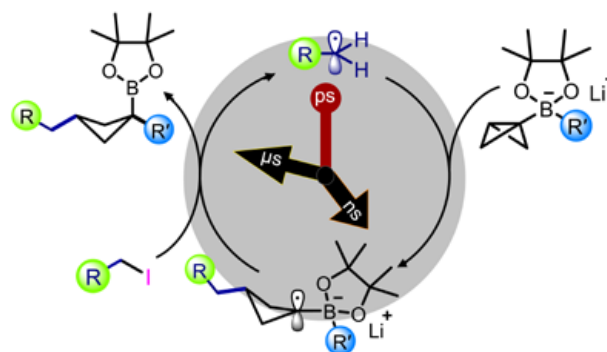
## Femtosecond to microsecond tracking of the complete mechanism of a radical reaction cycle

L. Lewis-Borrell, M. Sneha, V. Fasano, A. Noble, V.K. Aggarwal, A.J. Orr-Ewing (School of Chemistry, University of Bristol, Bristol, UK)

Chemical reactions driven by light are increasingly being used in synthetic chemistry, because they can efficiently access new chemical structures, but the reaction pathways are often difficult to understand. The absorption of ultraviolet or visible light produces short-lived reactive intermediates which drive the chemistry. Time-resolved infrared (TRIR) spectroscopy can observe these transient intermediates directly, track the timescales for their formation and loss, and hence unravel complicated reaction mechanisms.

The wide range of timescales for different reaction steps presents a challenge, with the initial radical formation occurring on femtosecond to picosecond timescales, but subsequent reaction steps extending out to microseconds or milliseconds. The extraordinary capability of the LIFETIME Facility to record TRIR spectra at intervals spanning ten orders of magnitude of time now makes this type of investigation possible. For the first time, complete mechanisms of a multi-step reaction can be tracked and understood.

Contact: A.J. Orr-Ewing (a.orr-ewing@bristol.ac.uk)



Schematic representation of the timescales over which the studied chemical reactions occur